

## Room temperature GaAs exciton-polariton light emitting diode

S. I. Tsintzos,<sup>1,2,a)</sup> P. G. Savvidis,<sup>1,2</sup> G. Deligeorgis,<sup>2</sup> Z. Hatzopoulos,<sup>3</sup> and N. T. Pelekanos<sup>1,2</sup>

<sup>1</sup>Department of Materials Science and Technology, University of Crete, P.O. Box 2208, 71003 Heraklion, Greece

<sup>2</sup>Microelectronics Research Group, IESL-FORTH, P.O. Box 1385, 71110 Heraklion, Greece

<sup>3</sup>Department of Physics, University of Crete, P.O. Box 2208, 71003 Heraklion, Greece

(Received 17 December 2008; accepted 25 January 2009; published online 18 February 2009)

Room temperature GaAs polariton emission is demonstrated under electrical injection. Temperature and angle-resolved electroluminescence measurements on a polariton light emitting diode clearly show the persistence of Rabi splitting and anticrossing behavior at temperatures as high as 315 K. We show that by increasing the number of quantum wells in the structure, the cutoff temperature for the strong coupling regime can be pushed beyond room temperature, in good agreement with theory. Our results suggest that optimally designed GaAs microcavities are perfectly suited for room temperature polaritronics. © 2009 American Institute of Physics. [DOI: 10.1063/1.3082093]

Exciton polaritons are remarkable manifestations of exciton-photon interaction in resonant optical media, such as semiconductor microcavities (MCs). Owing to their composite light-matter nature, polaritons exhibit strong nonlinearities and their behavior is often governed by a distinctive bosonic character, which is responsible for a series of spectacular demonstrations such as stimulated scattering of polaritons,<sup>1</sup> polariton amplification,<sup>2-5</sup> condensation,<sup>6-8</sup> and polariton lasing.<sup>9-13</sup> From a device point of view, a particularly attractive feature of polaritons and of their use in lasers is the two orders of magnitude reduction of threshold carrier density compared to conventional semiconductor lasers demonstrated in optical experiments.<sup>14</sup> This makes polariton lasers extremely promising as ultralow threshold lasers or as low-power sources of coherent and nonclassical light.

Essential prerequisites to achieve a real-world electrically pumped polariton laser are to combine in the same MC device, (i) persistence of strong coupling under electrical injection up to room temperature, (ii) efficient population of  $k_{\parallel} \sim 0$  polariton states at the bottom of the trap, bypassing relaxation bottleneck effects. Clearly, the whole field of polaritronics could see unprecedented development should this technology become available. Here, we make important progress on the former issue, namely, we demonstrate that electrically pumped GaAs polaritons can emit light in the strong coupling regime at room temperature. It is interesting to note that, until recently, due to the smaller exciton binding energies, GaAs MCs were not considered a system of choice for room temperature polaritronics,<sup>5</sup> in spite of an early work by Houdré *et al.*<sup>15</sup> Instead, room temperature operation was pursued in semiconductor systems with large exciton binding energies such as II-VI,<sup>1,11</sup> GaN,<sup>16</sup> and organic<sup>17</sup> MCs. However, each of these systems still presents some real technological issues despite rapid progress in recent years. For instance, in the GaN system there are serious difficulties with the fabrication of distributed Bragg reflectors (DBRs), the giant internal fields, the poor *p*-type doping, and the overall material quality. On the other hand, organic MCs suffer from the low carrier mobilities and the strongly localized nature of excitons. Instead, recent demonstration of electrically

pumped GaAs polariton light emitting diodes (LEDs),<sup>18,19</sup> operating even at 240 K,<sup>20</sup> highlights the potential of GaAs MCs for real-world room temperature polariton-based applications in optoelectronics.

In this letter, we report the experimental realization of a GaAs polariton LED, which directly emits from polariton states at *room temperature* and beyond. The strong coupling regime is evidenced by the characteristic anticrossing of the polariton states observed in temperature and angle-resolved electroluminescence (EL) measurements. These results can be well accounted for using a simple coupled harmonic oscillator model and strongly suggest that the GaAs system is well suited for room temperature polaritronics, given the maturity of GaAs based technologies.

For this work, five MC samples were grown by molecular beam epitaxy on GaAs (001)  $n^+$  substrates. The bottom DBR consists of 21 periods of  $\lambda/4$  GaAs/AlAs, *n*-type doped to  $2 \times 10^{18} \text{ cm}^{-3}$ , whereas the top DBR consists of 17 periods of  $\lambda/4$  GaAs/AlAs, *p*-type doped to  $4 \times 10^{18} \text{ cm}^{-3}$ . The  $5\lambda/2$  GaAs cavity contains, depending on the targeted operating temperature, either three or four pairs of 10 nm  $\text{In}_{0.1}\text{Ga}_{0.9}\text{As}/\text{GaAs}$  quantum wells (QWs) placed at the antinodes of the electric field, as schematically depicted in Fig. 1(a). Each sample was designed to exhibit the strong coupling regime in a specific temperature window, covering the temperature range from 20 K up to room temperature or higher. To minimize the effects of the doping-related losses inside the cavity, the inner half period of each DBR was kept undoped.<sup>21</sup> Polariton LEDs were fabricated by using standard GaAs processing technology. In order to reduce the series resistance of the top *p*-DBR, the *p*-contacts are deposited following an Ohmic recess step. This way, the top 11 periods of the *p*-DBR are electrically bypassed. Ti/Pt *p*-type contacts were formed in a ring-shaped geometry with 100  $\mu\text{m}$  wide rings at the edge of the 400  $\mu\text{m}$  wide cavity mesas. For electrical isolation, the region between adjacent devices is etched by a second deeper reactive ion etching step, reaching down to the *n*-DBR. Finally, the *n*-type (Au/Ge) Ohmic contact was back-side evaporated. Ohmic contacts were activated by a rapid thermal annealing at 420 °C. In Fig. 1(b), a scanning electron microscopy (SEM) image from a completed polariton LED is presented.

<sup>a)</sup>Electronic mail: simostsi@physics.uoc.gr.

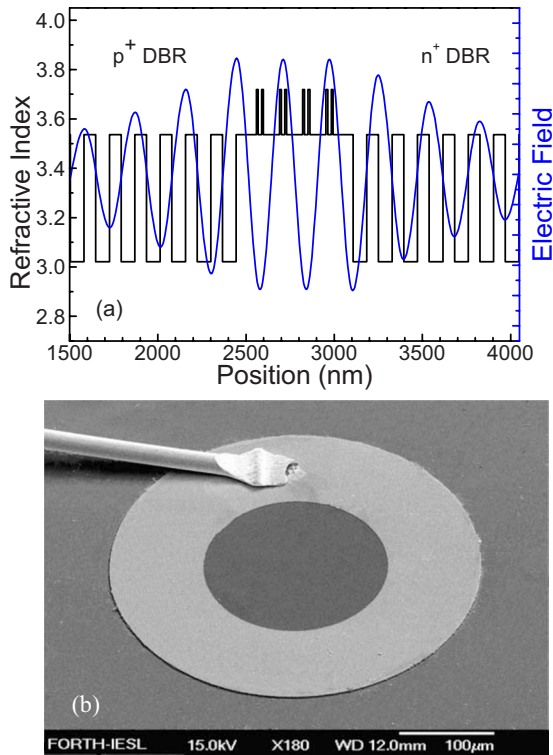


FIG. 1. (Color online) (a) Electric field and refractive index profile along the structure. The QWs are positioned at the maxima of the electric field to increase light matter coupling. (b) SEM photo of polariton LED.

To study the emission properties of our MC polariton LEDs under electrical injection, we used both temperature and angular measurements to tune the excitonic and cavity modes with respect to each other, searching for the characteristic anticrossing between the two modes. Figure 2(a) shows EL spectra collected at zero angle for different temperatures in the range of 260–320 K from a polariton LED containing four pairs of QWs, exhibiting the characteristic anticrossing behavior.<sup>20</sup> The energy dispersion curves of the upper and lower polaritons are shown in Fig. 2(b). The data points are extracted from the EL peaks in Fig. 2(a), while the solid lines are theoretical fits generated by applying a coupled harmonic oscillator model to our data.<sup>22</sup> An excellent fitting of the upper and lower polariton branches is obtained demonstrating that EL at these high temperatures arises from exciton-polariton states in the strong coupling regime. The normal mode Rabi splitting is found to be 4 meV at 288 K.

To test the endurance of polariton LED emission at even higher temperatures, we performed angle-resolved EL measurements on a polariton LED sample with four pairs of QWs, which was designed to exhibit strong coupling at  $T > 300$  K. In Fig. 3(a), we present selected angle-resolved EL spectra obtained at  $T = 315$  K under electrical injection of 0.52 mA ( $\sim 0.54$  A/cm<sup>2</sup>), from a diode with a negative detuning of 11.5 meV at zero angle. The corresponding energy dispersion curves of the upper and lower polaritons are shown in Fig. 3(b), exhibiting a clear anticrossing at  $\sim 30^\circ$  with a 4 meV Rabi splitting, thus demonstrating that the strong coupling regime persists even at 315 K. Using this value for the Rabi splitting, the upper and lower polariton dispersion curves are reproduced very well (solid lines), using the coupled harmonic oscillator model mentioned above.

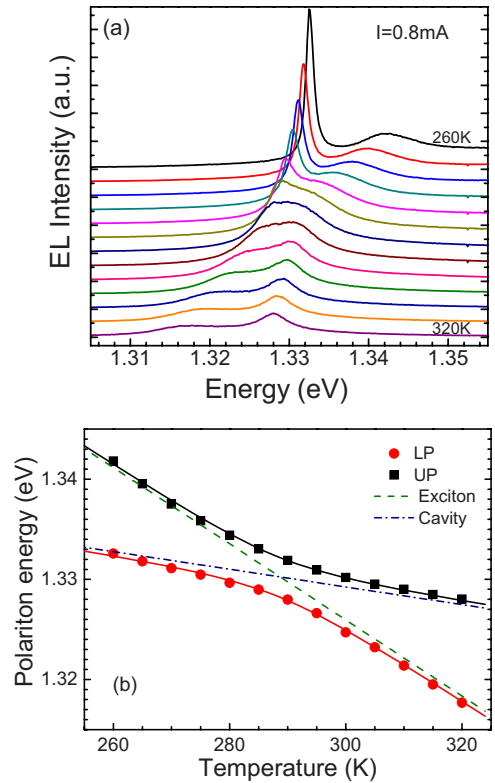


FIG. 2. (Color online) (a) EL spectra recorded from a polariton LED at zero angle for different temperatures between 260 and 320 K, with a step of 5 K. (b) Polariton energy dispersion. The data points are extracted EL peaks and the solid lines are fits for the upper and lower polariton branches.

In depth understanding of why GaAs polariton LEDs are capable of operating in the strong coupling regime at high temperatures can be inferred from Fig. 4, where all zero-detuning Rabi splittings measured in this work from various polariton LEDs as a function of temperature are plotted. Each data point is extracted from a set of temperature dependent EL experiments under normal collection, as is the case of Fig. 2. The data points are grouped into a set of circles corresponding to MCs with six QWs ( $N = 6$ ) and to a set of squares for MCs with eight QWs ( $N = 8$ ). Clearly, the Rabi splitting increases with the number of QWs and decreases with temperature. To account for these results, we employ a simplified model, calculating the zero-detuning Rabi splitting in the strong coupling regime using the equation<sup>22</sup>  $\Omega(T) = \sqrt{4V^2 - (\gamma_{\text{ex}}(T) - \gamma_c)^2}$ . The parameter  $V$  represents the coupling strength between the cavity photon mode and the exciton and is expected to be proportional to  $N^{1/2}$ , while  $\gamma_{\text{ex}}$  and  $\gamma_c$  are the exciton and photon linewidths, respectively. The expression in the square root has to remain positive, which is a precondition for the strong coupling regime.<sup>22</sup> In this model, the temperature dependence of  $\Omega(T)$  comes solely through the exciton linewidth,  $\gamma_{\text{ex}}(T) = \gamma_{\text{inh}} + \gamma_{\text{ac}}T + \gamma_{\text{LO}}[\exp(\hbar\omega_{\text{LO}}/kT) - 1]^{-1}$ , where  $\gamma_{\text{inh}}$  is the low temperature inhomogeneous linewidth,  $\gamma_{\text{ac}}$  and  $\gamma_{\text{LO}}$  are constants representing the strength of exciton coupling with acoustic and LO phonons, respectively, and  $\hbar\omega_{\text{LO}}$  is the LO phonon energy.<sup>23</sup> To experimentally determine  $\gamma_{\text{ex}}$ , we performed transmittance measurements on a separate sample containing two InGaAs/GaAs QWs identical to those used in our MC structures. In the inset of Fig. 4, the measured exciton linewidth as a function of temperature is depicted. The solid line

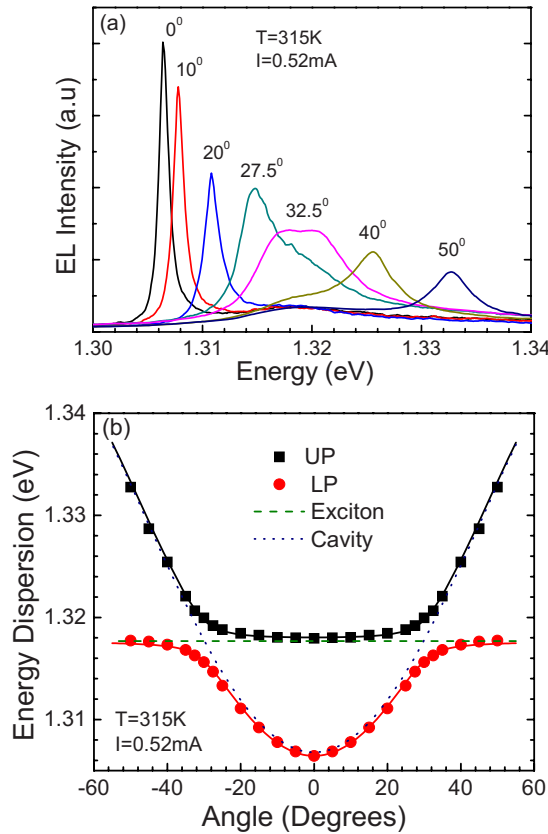


FIG. 3. (Color online) (a) Selected EL spectra at various angles for 0.52 mA at 315 K. (b) Polariton energy dispersion curves vs collection angle. The circular and square points are extracted EL peaks while the solid lines are theoretical fittings.

running through the experimental points was obtained by fitting the equation for  $\gamma_{\text{ex}}(T)$  to our results, using  $\gamma_{\text{ac}} = 4.4 \mu\text{eV/K}$  and  $\gamma_{\text{LO}} = 15.2 \text{ meV}$ . It should be noted that these values are in excellent agreement with those given by Gammon *et al.*<sup>23</sup> for similar InGaAs/GaAs QWs. Using these values for  $\gamma_{\text{ex}}(T)$  and taking  $\gamma_c = 1 \text{ meV}$ , directly measured in off-resonance zero-collection angle conditions, we fit both sets of data points by applying the equation for  $\Omega(T)$  and using  $V(N)$  as the only adjustable parameters. The solid lines running through the data points are best fits obtained for

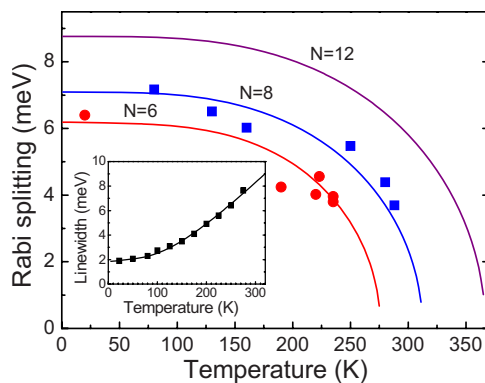


FIG. 4. (Color online) Comparison of theoretical and experimental zero-detuning Rabi splitting as a function of temperature. The circular points refer to MCs with six QWs, while the squares to MCs with eight QWs. Solid lines are theoretical curves for 6, 8, and 12 QWs. The inset shows the temperature dependence of the exciton full width at half maximum linewidth extracted from transmission measurements.

$V(6) = 3.13 \text{ meV}$  and  $V(8) = 3.63 \text{ meV}$ , which scale according to  $V(N) \sim N^{1/2}$  as expected. As we can see from Fig. 4, our model describes quite well the temperature behavior of the experimental Rabi splittings and confirms the ability of polaritonic emission from a GaAs system at room temperature. Another important point of Fig. 4 is that by increasing the number of the QWs to  $N = 12$ , the operating temperature of the polariton LED can be extended up to 340 K.

To summarize, in this letter we report a clear demonstration of a GaAs polariton LED operating at room temperature. The strong coupling regime at these elevated temperatures is revealed by the characteristic anticrossing between the two polariton branches observed in temperature and angle resolved EL experiments. These findings are important because they open the way toward practical polariton emitters, based on the well established GaAs technology.

The support by the PENED national projects under Project Nos. 03EΔ841 and 03EΔ816 is acknowledged.

<sup>1</sup>L. S. Dang, D. Heger, R. André, F. Bœuf, and R. Romestain, *Phys. Rev. Lett.* **81**, 3920 (1998).

<sup>2</sup>P. G. Savvidis, J. J. Baumberg, R. M. Stevenson, M. S. Skolnick, D. M. Whittaker, and J. S. Roberts, *Phys. Rev. Lett.* **84**, 1547 (2000).

<sup>3</sup>C. Ciuti, P. Schwendimann, B. Deveaud, and A. Quattropani, *Phys. Rev. B* **62**, R4825 (2000).

<sup>4</sup>C. Ciuti, P. Schwendimann, and A. Quattropani, *Phys. Rev. B* **63**, 041303 (2001).

<sup>5</sup>M. Saba, C. Ciuti, J. Bloch, V. Thierry-Mieg, R. André, L. S. Dang, S. Kundermann, A. Mura, G. Bongiovanni, J. L. Staehli, and B. Deveaud, *Nature (London)* **414**, 731 (2001).

<sup>6</sup>J. J. Baumberg, P. G. Savvidis, R. M. Stevenson, A. I. Tartakovskii, M. S. Skolnick, D. M. Whittaker, and J. S. Roberts, *Phys. Rev. B* **62**, R16247 (2000).

<sup>7</sup>R. M. Stevenson, V. N. Astratov, M. S. Skolnick, D. M. Whittaker, M. Emam-Ismaïl, A. I. Tartakovskii, P. G. Savvidis, J. J. Baumberg, and J. S. Roberts, *Phys. Rev. Lett.* **85**, 3680 (2000).

<sup>8</sup>C. Diederichs, J. Tignon, G. Dasbach, C. Ciuti, A. Lemaitre, J. Bloch, Ph. Roussignol, and C. Delalande, *Nature (London)* **440**, 904 (2006).

<sup>9</sup>D. Porras, C. Ciuti, J. J. Baumberg, and C. Tejedor, *Phys. Rev. B* **66**, 085304 (2002).

<sup>10</sup>G. Malpuech, A. Di Carlo, and A. Kavokin, *Appl. Phys. Lett.* **81**, 412 (2002).

<sup>11</sup>J. Kasprzak, M. Richard, S. Kundermann, A. Baas, P. Jeambrun, J. M. J. Keeling, F. M. Marchetti, M. H. Szymanska, R. André, J. L. Staehli, V. Savona, P. B. Littlewood, B. Deveaud, and L. S. Dang, *Nature (London)* **443**, 409 (2006).

<sup>12</sup>H. Deng, D. Press, S. Götzinger, G. S. Solomon, R. Hey, K. H. Ploog, and Y. Yamamoto, *Phys. Rev. Lett.* **97**, 146402 (2006).

<sup>13</sup>L. Butov, *Nature (London)* **447**, 540 (2007).

<sup>14</sup>H. Deng, G. Weihs, D. Snoke, J. Bloch, and Y. Yamamoto, *Proc. Natl. Acad. Sci. U.S.A.* **100**, 15318 (2003).

<sup>15</sup>R. Houdré, R. P. Stanley, U. Oesterle, M. Illegems, and C. Weisbuch, *Phys. Rev. B* **49**, 16761 (1994).

<sup>16</sup>S. Christopoulos, G. Baldassarri Höger von Högersthal, A. J. D. Grundy, P. G. Lagoudakis, A. V. Kavokin, J. J. Baumberg, G. Christmann, R. Butté, E. Feltn, J. F. Carlin, and N. Grandjean, *Phys. Rev. Lett.* **98**, 126405 (2007).

<sup>17</sup>J. R. Tischler, M. S. Bradley, V. Bulovic, J. H. Song, and A. Nurmikko, *Phys. Rev. Lett.* **95**, 036401 (2005).

<sup>18</sup>D. Bajoni, E. Semenova, A. Lemaitre, S. Bouchoule, E. Wertz, P. Senellart, and J. Bloch, *Phys. Rev. B* **77**, 113303 (2008).

<sup>19</sup>A. A. Khalifa, A. P. D. Love, D. N. Krizhanovskii, M. S. Skolnick, and J. S. Roberts, *Appl. Phys. Lett.* **92**, 061107 (2008).

<sup>20</sup>S. I. Tsintzos, N. T. Pelekanos, G. Konstantinidis, Z. Hatzopoulos, and P. G. Savvidis, *Nature (London)* **453**, 372 (2008).

<sup>21</sup>S. I. Tsintzos, P. G. Savvidis, G. Konstantinidis, Z. Hatzopoulos, and N. T. Pelekanos, *Phys. Status Solidi* **5**, (c), 3594 (2008).

<sup>22</sup>A. V. Kavokin, J. J. Baumberg, G. Malpuech, and F. P. Laussy, *Microcavities* (Oxford University Press, New York, 2007).

<sup>23</sup>D. Gammon, S. Rudin, T. L. Reinecke, D. S. Katzer, and C. S. Kyono, *Phys. Rev. B* **51**, 16785 (1995).